ELSEVIER

Polymer 40 (1999) 2929–2938

polymer

Relationship between surface and bulk morphologies for immiscible polymer blends

G. Verfaillie*, J. Devaux, R. Legras

Unité de Physique et de Chimie des Hauts Polymères, Croix du Sud, 1, B-1348 Louvain-la-Neuve, Belgium

Received 14 November 1997; revised 30 March 1998; accepted 29 April 1998

Abstract

The surface morphology of compression-moulded PP/PET blends is investigated and compared to the bulk morphology. Before compression moulding the blends are prepared by melt mixing in a Brabender plastograph. Model experiments are developed to analyse the influence of the processing conditions and of the nature of the moulding surface on the surface and bulk morphologies. Films are prepared under different shear conditions with PI as the moulding surface. At low shear rates the bulk and surface morphologies (size and composition) are very similar. At high shear rates and when the PET is the dispersed phase, the nodules at the surface are highly deformed in the flow direction while the PET nodules remaining in the bulk are undeformed. The PET concentration at the surface increases above the bulk concentration. When PP is the dispersed phase, the surface concentration is much lower than the bulk concentration. The observed surface morphology for samples prepared with high shearing can be explained by an interplay between the flow field and the affinity of the dispersed phase for the moulding surface.

Keywords: Surface morphology; Bulk morphology; PP/PET blends

1. Introduction

Polymer blending is now an important field in polymer research and has given many years to the development of materials with synergetic properties. Most of the polymers are immiscible at the molecular scale. Due to chain connectivity, the entropy of mixing is very low and without specific interactions, biphasic systems result from melt mixing. Many studies have dealt with the control of the phase dispersion in polymer blends. The bulk morphology created by melt mixing is shown to depend on parameters such as: shear rate, viscosity, viscosity ratio, elasticity, elasticity ratio, interfacial tension reactivity of functional groups and mixing time [1–11].

However, less is known about parameters controlling the surface properties. Surface properties are important for biocompatibility [12–15] or adhesion [16] and receive increasing attention in literature. Theoretical [17–20] and experimental [21–31] studies on miscible polymer blends showed that for miscible blends at equilibrium an enriched surface layer of the lower surface tension component exist with a concentration gradient towards the bulk. The extent of the surface enrichment depends on the difference in surface free energy, on the interaction between the polymers and on the molecular weights. Experimentally, the surface concentration is also shown to be influenced by kinetic parameters such as solvents used for blending [23], thermal history [21,29,31] and changes in bulk thermodynamics (crystallization of one of the phases) [25,26].

For immiscible (phase-separated) blends the literature gives examples where most of the time samples are prepared by solvent casting or spin coating generally followed by annealing [21,24,32–41]. Most of the results indicate that one of the driving forces behind the surface enrichment of one phase is the difference in surface tension between the constituents.

For PS/PMMA solution prepared blends the surface was shown to be heterogeneous [38–41]. The surface and bulk morphology resulting from a phase separation is also dependent on: the blending solvent, the speed of evaporation, sample thickness and the substrate polarity. For phase-separated PVC/PMMA blends casted from THF [32–37], it is shown by XPS and ToF-SIMMS analysis that the surface is covered with a fine film of PMMA with a thickness of the order of 1 nm. Underneath this film a heterogeneous blend is found.

One of the few surface studies dealing with immiscible polymer blends prepared by melt mixing has been attempted

* Corresponding author.

0032-3861/99/$ - see front matter
PII: S0032-3861(98)00336-X

by Bhatia et al. [42]. They studied injection-moulded samples of PPE/PA and blends. By XPS they find the surface to be matrix dominated. Compatibilization of the PPE/PA blend decreases the surface enrichment by the matrix. The structure of the copolymer influences the extent of this decrease.

The scope of the present work is to analyse the surface morphology of immiscible blends after melt processing in relation with the bulk morphology. In a previous paper [43] we reported on the surface analysis of a PP/PET 28/72 blend compression moulded on a PT surface. At this volume fraction, PP is the dispersed phase. The surface analysing techniques used are time of flight secondary ion mass spectroscopy (ToF-SIMS), lateral force microscopy (LFM) and scanning electron microscopy (SEM). The three techniques reveal the same heterogeneities at the surface, showing PP nodules in the PET matrix with sizes ranging from 1 to 100 μm. ToF-SIMS images recorded with ions characteristic for PET ($C_6H_4^+$, $C_7OH_4^+$, $C_8O_3H_5^+$,O^- and OH^-) allow a chemical mapping of the surface. In LFM, the contrast can be associated with the difference in the nature and/or the physico-chemical properties of the polymers present at the surface (matrix and dispersed phase). We further conclude that for a systematic approach of the problem SEM is the most valuable tool for the surface analysis of PP/PET blends.

This work reports on the influence of blend composition, flow rate during processing on the surface and bulk morphologies of the PP/PET blend.

2. Experimental

2.1. Melt mixing and preparation of heterogeneous surfaces

Blends of poly(propylene) (PP Shell SS6500) and poly(ethyleneterephthalate) (PET ICI B90L) are prepared in a Brabender plastograph W-50EH. The experimental conditions are reported in Table 1. Thermal degradation of PP is limited by the addition of 2% of Irganox 1010. The volume percentages mentioned in Table 1 are calculated from the weight fraction. The specific masses of both products are determined by means of a pycnometer and methanol at 25°C. The specific masses measured are 0.9 g cm^{-3} and 133 g cm^{-3} for PP and PET, respectively.

Compression moulding is performed with a Fontijne press type SRA 100. The experimental conditions are given in Table 1. The blends are placed in an aluminium mould of 0.01 cm thickness. Throughout all of the work the surface in contact with the polymer is a polyimide film (PI) supplied by ASF. The mould is placed in the press at 280°C and the blend is melted during 1 min, after which a pressure of 1.64 MPa (10 t on a surface of 0.2×0.3 m^2) is applied to the mould for 15 s. The pressure is then maintained during various times. After compression moulding the samples are annealed during different times at atmospheric pressure. After annealing, the compression-moulded films are quenched in water at room temperature.

In order to analyse the influence of the flow during the compression moulding two different starting shapes were used for moulding. To minimize the flow in during compression moulding, the blend after melt mixing is ground into powder. A high speed grinder (Pulverisette-FRITSCH—15 000 rpm, 200 μm mesh) and liquid nitrogen are used. The size of the grains is of the same order of magnitude as the thickness of the mould. The powder is then homogeneously spread over the entire surface of the mould and melted prior to pressurization of the mould. In this way we obtain samples at low shear. To maximize the flow to during compression moulding blocks of the necessary mass were cut from the solidified Brabender content and placed in the middle of the mould. These blocks are then squeezed after melting. The squeezing of the molten polymer allows us to obtain samples at high shear (rate) during the compression moulding.

Table 1
Processing conditions for the PP/PET blends

Melt mixing in BRABENDER	
PP/PET (volume%)[a]	14.5/21/28/34/40.0/50.5/60.5/70/78/86/93
Temperature (°C)	280
rotation speed (rpm)	50
Mixing time (min)	5
Amount Irganox 1010%	2
Mixing atmosphere	N2
Cooling	air
COMPRESSION MOULDING of films	
Temperature (°C)	280
Melting time (min)	1
Moulding time under pressure (min)	2, 3, 5, 10
Annealing time at 280°C (min)	0, 1, 5
Pressure (MPa)	1.6
Cooling	H_2O at 20°C
Moulding surface	Polyimide (PI)

[a] The volume percentage given is calculated from the weight fraction added with the densities of PP and PET being 0.9 and 1.34 g cm^{-3}.

The samples' processing conditions are reported with the following notations: PP/PET $c/(100-c)$ P $x/y/z$, where PP/PET ($c/100-c$) stands for a PP/PET blend containing c% PP by volume and P $x/y/z$ stands for a film prepared from powder (P) for which the melting time is x min, the moulding time under pressure y min and the annealing time z min. For the squeezing flow experiment, when the blocks are used directly after Brabender mixing, B is used.

2.2. IR spectroscopy

The bulk concentration (C_b) of the dispersed phase after grinding has been measured by means of IR spectroscopy. The FT-IR spectrometer used is a Perkin Elmer FTIR 1760-X. Spectra are recorded between 4000 and 400 cm^{-1}, averaged over 10 scans, with a resolution of 1 cm^{-1}. The absorption bands used for calibration are 2723 cm^{-1} for PP and 1950 cm^{-1} for PET. Using the Lambert–Beer law the PP concentration can be written as a function of the absorbency at these wavelengths as:

$$A_{rel} = \frac{A_{2723PP}}{A_{2723PP} + A_{1950PET}} = \frac{C_{pp}\varepsilon_{pp}t}{C_{pp}\varepsilon_{pp}t + C_{pet}\varepsilon_{pet}t} \quad (1)$$

$$C_{pp} = \frac{A_{rel}\varepsilon_{pet}}{(\varepsilon_{pp}(1-A_{rel}) + A_{rel}\varepsilon_{pet})} \quad (2)$$

where A_{rel}, A, C, ε and t are, respectively, the relative absorbance, the absorbance, bulk concentration, the extinction coefficient and the thickness of the films, with obvious indices.

The extinction coefficients for the absorption bands at 2723 cm^{-1} for PP and 1950 cm^{-1} and PET are determined by measuring the absorption as a function of the thickness of pure PP and PET films. The slope of the linear regression between thickness and absorption gives direct access to this coefficient. The extinction coefficients obtained are 0.0031 cm^{-1} and 0.0037 cm^{-1} for PP and PET, respectively, at 2723 cm^{-1} and 1950 cm^{-1}. The correlation coefficient of the fittings are 0.9995 and 0.9994 for PP and PET, respectively.

2.3. SEM and image analyses

The scanning electron microscope used is a Hitachi S-570. The samples are covered with a 15 nm thick layer of AuPd. The sputtering device used is a Balzers Union SCD 040. The images are treated with a Kontron image analyser equipped with the IBAS-II system. The contrast (grey levels) is not sufficient to carry out an automatic analysis. Every image has to be hand-treated, by approximating the contours by circles or polygons.

Bulk morphology is determined on cryogenically fractured surfaces. The number average diameter of the dispersed phase (D_b) is obtained by analysing three different zones including at least 200 measured nodules.

Table 2
The polar (γ_p) and disperse component (γ_d) of the surface tension ($\gamma = \gamma_p + \gamma_d$) of PP, PET and PI

	Surface energy: disperse component γ_d (N m^{-1})	Surface energy: polar component γ_p (N m^{-1})
H_2O	29.2 ± 0.1	42.7 ± 0.1
1α-Bromonaphthalene	44.4 ± 0.3	0.0 ± 0.1
PP	34.4 ± 0.4	5.6 ± 0.5
PET	44.2 ± 0.1	13.5 ± 0.4
PI	43.2 ± 0.2	23.4 ± 0.3

The surface images of the compression-moulded films are obtained with the SEM working at an acceleration voltage of 15 keV. The surface analysis is performed on three samples analysed each on three zones of 1 cm^2. On each of these zones, six or more pictures are systematically taken. On each of these pictures the average diameter at the surface (D_s) and number of particles per unit area are determined. The surface concentration (C_s) is obtained from the average nodular area at the surface multiplied with the number of nodules per unit area at the surface.

2.4. Surface energy measurements

The surface energy of the polymers is determined by means of contact angles of water and α-bromonaphthalene. These were measured with a video camera and an image analysis system (Electronisch Ontwerpsbureau De Boer, The Netherlands) providing an evaluation of the contact angle at the triple point and its deduction from the height and the width of the drop [44,45]. The drop volume was 0.3 μl. The surface energy (γ) was deduced from the contact angles, using the Wu harmonic-mean equation [46]:

$$\gamma_l(1+\cos\theta) = 4\left(\frac{\gamma_l^d+\gamma_s^d}{\gamma_l^d\gamma_s^d}\right) + 4\left(\frac{\gamma_l^p+\gamma_s^p}{\gamma_l^p\gamma_s^p}\right) - \pi e \quad (3)$$

where πe is the spreading pressure, the subscripts l and s refer to the liquid and the solid, respectively, and the exponents d and p refer to the dispersion and polar contributions, respectively.

α-Bromonaphthalene was considered to have only dispersion interactions with the surface. The surface tension of the liquids are given in Table 2. They are obtained by means of a reference surface, PARAFILM®, on which the surface energy is entirely determined by dispersion interactions.

3. Results and discussion

3.1. IR calibration

The relative absorbance is measured for films over the entire composition range for samples prepared from powder and pieces corning from the Brabender. In Fig. 1 the measured PP concentration in the films is given as a function

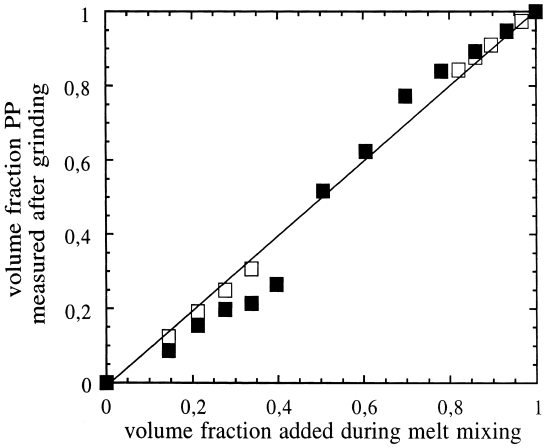

Fig. 1. The PP measured concentration as a function of the added PP concentrations in the blend. The graph compares films prepared by powder and pieces coming from the Brabender where the symbols used are: ■ for PP/PET *x*/1-*x P* and □ for PP/PET *x*/1-*x B* blends.

of the added concentration. The measured concentration is obtained from Eq. (2). For samples prepared from powder a deviation between the added and measured concentration is found. This deviation corresponds to a loss in dispersed phase. PP and PET are highly incompatible, leading to poor interfacial adhesion. During cryogenic grinding of the blend, fracture surfaces are created. In this way nodules are exposed to the surface and lost during the grinding. When PP is the dispersed phase the loss is larger than when PET is the dispersed phase. Going further in the explanation presented above of nodule losses, this can be understood from the difference in thermal expansion coefficients. The thermal expansion coefficient of PP is larger than for PET considering the fact that the samples are quenched sufficiently fast to prevent PET from crystallizing [47]. During the rest of the work the bulk concentration used will be the measured concentrations.

3.2. Compression moulded PP/PET films at low shear

3.2.1. Variation of blend composition at constant processing conditions

The influence of blend composition on the surface morphology has been analysed for films prepared from melt-mixed blends ground into powder. The shear exerted on the system during melt mixing remains low. In this section, for all films, the melting time is 1 min, the moulding time under pressure is 2 min and the time of annealing 0 min (PP/PET $x/1-x$ *P* 1/2/0). Fig. 2a, c, e shows typical SEM images of the surface of the following systems: PP/PET 28/72, 86/14 and 50/50 *P* 1/2/0. Fig. 2b, d, f shows fractured surfaces exhibiting the bulk morphology of the respective blends. At low PP concentration, PP forms the dispersed phase (e.g. PP/PET 28/72) and at high PP concentration, PET is the dispersed phase (e.g. PP/PET 86/14). One can see in Fig. 2a–d that when the bulk morphology is nodular the surface morphology remains spherical. In between these

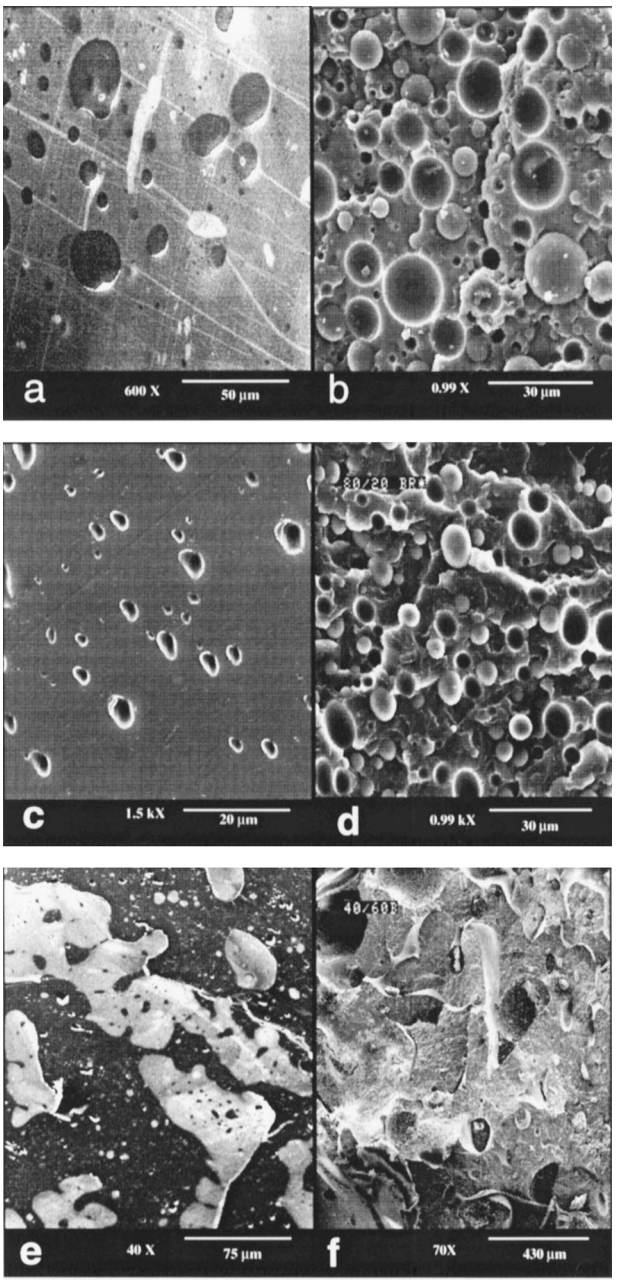

Fig. 2. SEM images taken on the surface of compression-moulded films of (a) PP/PET 28/72 *P* 1/2/0, (c) PP/PET 86/14 *P* 1/2/0, (e) PP/PET 50/50 *P* 1/20 and on fractured blends showing the bulk morphology of (b) PP/PET 28/72, (d) PP/PET 86/14, (f) PP/PET 50/50.

concentration regions a phase inversion occurs. Fig. 2e, f shows that both the bulk morphology and the surface morphology are cocontinuous.

In the case where PET is the dispersed phase (Fig. 2c) the lack of adhesion between PP and PET and the sticking of PET to the PI moulding surface leads to the retention of most of the PET nodules on the PI film. In these conditions the surface morphology presents holes instead of PET nodules. In the following the size and concentration of dispersed PET at the surface are obtained from analysing the holes left by PET.

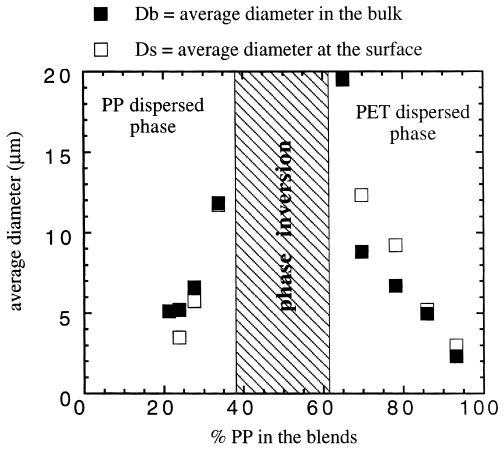

Fig. 3. Size of the dispersed phase at the surface and in the bulk as a function of blend compositions where ■ is the average diameter in the bulk and, □ is the average diameter at the surface.

For all the systems, image analysis of the micrographs has been performed (Fig. 2 a, c, e). The average size and concentration of the dispersed phase at the surface are determined as a function of bulk composition. Fig. 3 gives the dispersed phase size in the bulk (nodule diameter: D_b) and at the surface (D_s) as a function of the bulk PP volume concentration. As explained in the experimental section, the bulk concentration (C_{pp}) is corrected for the loss in dispersed phase by means of IR spectroscopy.

The concentration region for phase inversion is situated between 40 and 60% PP. This concentration region is the same for both the bulk and surface of the blends. The diameter in the bulk follows the experimental relation with $C + C^2$ as determined by Favis et al. [3]. The dispersed phase size at the surface is larger than in the bulk when PET is the dispersed phase and smaller when PP is the dispersed phase. Fig. 4a, b shows the bulk and the surface morphology of films fractured for both systems (Fig. 4a: PP/PET 86/42 *P* 1/2/0 and Fig. 4b: 28/72 *P* 1/2/0). In Fig. 4b a PP nodule is shown emerging at the surface while Fig. 4a shows a hole left by a PET. This behaviour can be explained by the interfacial tension difference between the different constituents: PP, PET and the moulding surface PI. Direct access to the interfacial energy values at the processing temperature is difficult. However, the surface energy at room temperature of the different polymers (PI, PP and PET) gives a qualitative image of the interfacial tension. Effectively (i) the magnitude of difference in polarity expresses primarily the interfacial tension between two phases and (ii) the polar part of the surface tension is roughly independent of temperature [48].

Table 2 gives the polar and the dispersion components of the surface energy of the polymers. The absolute value of the surface energy is dependent on the experimental conditions and theoretical frame used. The values have therefore to be used only in a comparative way. The polarities of PET and PI are much higher than that of PP. The interfacial tension between PP and PI is thus higher than that between PET and PI. This explains the large contact angles of PP nodules with the PI surface, the nodules being dispersed in a PET matrix.

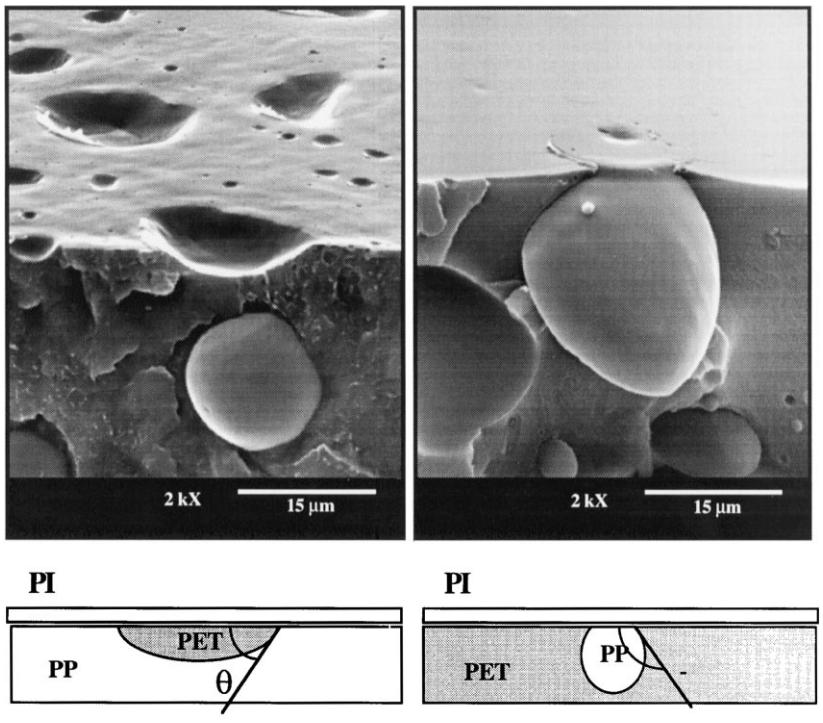

Fig. 4. Fractured films of PP/PET 86/14 *P* 1/2/0 and PP/PET 28/72 *P* 1/2/0. The figures show nodules (or holes left by nodules) present at the surface of the bulk (*P*1). The contact angle θ taken by the dispersed phase is influenced by its affinity for the moulding surface.

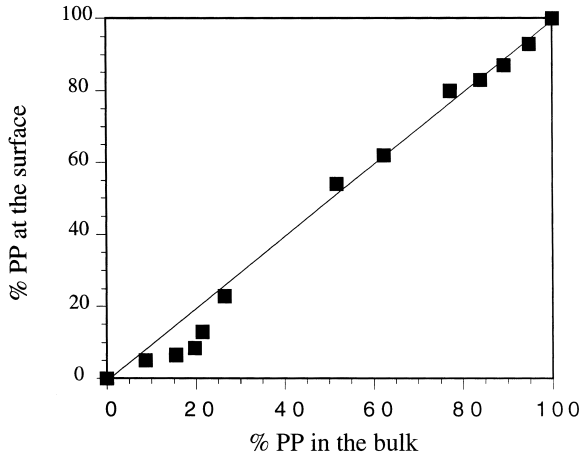

Fig. 5. Surface concentration as a function of bulk concentration where ■ is PP/PET *P*.

Fig. 5 reports the variation of the surface concentration as a function of the PP volume fraction (corrected for the loss of dispersed phase during grinding).

It is observed that when PET is the dispersed phase the bulk concentration is very close to the surface concentration.

On the other hand, when the PP is the dispersed phase, its surface concentration is much lower than in the bulk. To explain the deviation from linearity between surface and bulk concentrations in the composition range where PP is the dispersed phase, a theoretical surface concentration is calculated. The nodule cross-section in the bulk multiplied by the number of nodules per unit area at the surface gives the concentration that would be present at the surface, if the dispersed phase had the same diameter at the surface as in the bulk ($C_s d_b$). The value of $C_s d_b$ now is used in comparison with the experimentally determined surface concentration (C_s). Table 3 gives C_s and $C_s d_b$ at three different PP concentrations in the bulk (C_b). The $C_s d_b$ is closer to the surface concentration C_s than to the bulk concentration (C_b). Thus there is a lower number of nodules per unit area at the surface than in the bulk. If the $C_s d_b$ value would have been equal to C_b the difference in surface and bulk concentration could have been attributed to the difference in size. Now the difference in concentration is not only caused by difference in size. Therefore, to explain the lower number of nodules per unit area at the surface than in the bulk, a deeper investigation of the starting morphology and the mechanisms of compression moulding is necessary.

Table 3
Surface concentration of PP/PET blends with PP as dispersed phase

C_b^a (%)	C_s^b (%)	$C_s d_b^c$ (%)	D_b^d (μm)	D_s^e (μm)
15.4	6.9	9.4	5.2	3.48
19.7	8.4	9.6	6.6	5.75
21.5	13.0	13.2	11.8	11.7

[a] C_b = blend bulk PP concentration (%); [b] $C_s d_b$ = surface concentration PP if the average diameter at the surface was the same as in the bulk (%); [c] C_s = surface concentration PP (%); [d] D_s = measured average diameter at the surface (μm); [e] D_b = average diameter in the bulk (μm).

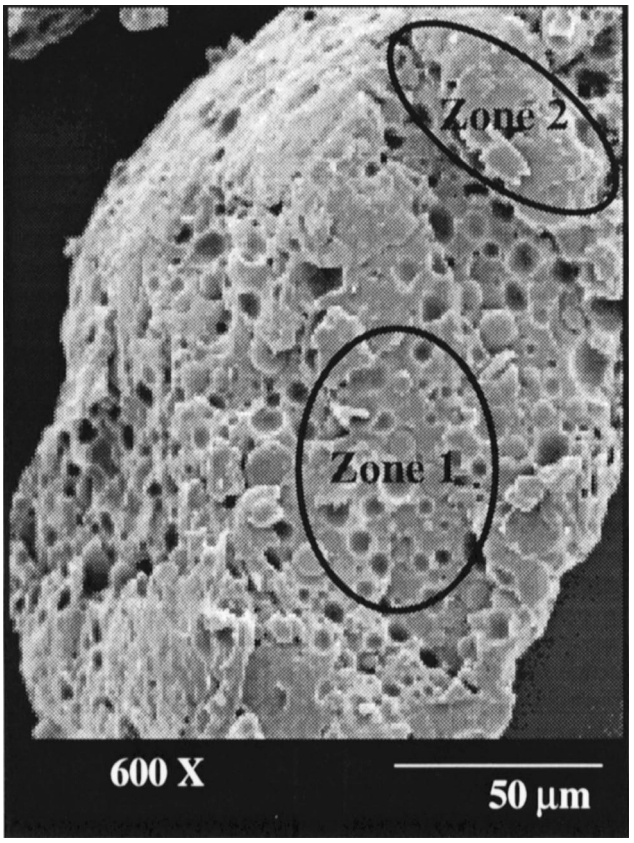

Fig. 6. SEM image of the surface of the ground powder of a PP/PET 28/72 Zone 1: fracture surface on grain, Zone 2: non-fracture surface.

Fig. 6 SEM shows the surface of the ground powder of a PP/PET 28/72 blend. Two different zones can distinguished: first (zone 1) a fracture surface where the dispersed phase is

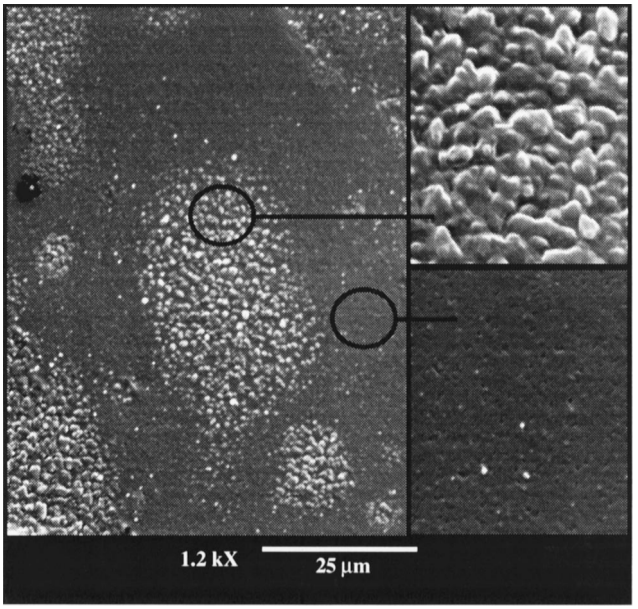

Fig. 7. Image of the surface of the blend (PP/PET 86/14 *P* 1/0/0) melted for 1 min without applying pressure on the mould.

exposed and, secondly (zone 2), non-fractured zones where no dispersed phase is present at the surface. Because grinding leaves a small amount of non-fractured surface an important loss can take place at the fracture surface.

The surface heterogeneity of the ground powder is clearly shown in Fig. 7. It shows the surface of a sample obtained from melting this powder for 1 min (PP/PET 78/22 *P* 1/0/0). No pressure was applied to the molten polymer. The powder was homogeneously spread in the mould. Zones of high and low concentrations of dispersed phase can be clearly distinguished on the micrograph. When pressure is applied, the flow in the mould is very low and zones with different concentrations of dispersed phase are still visible.

The loss of dispersed phase during grinding is more important when PET is the matrix (Fig. 1b). This explains, in our opinion, the difference in concentration in the bulk and at the surface after compression moulding under the experimental conditions (Fig. 5).

3.2.2. Variation of processing conditions at constant blend compositions

The objective of this section is to investigate the influence of processing time on the surface morphology. First the bulk morphology has been examined as a function of time at 280°C under static conditions. The results are reported in Fig. 8 for PP/PET 86/14 and 28/72 blends. The increase of the bulk phase size during the investigated time scale remains small. Theoretical and experimental results have already shown that the behaviour is related to the polymer's high viscosity [49,50].

In this series of experiments, the dispersed phase size and concentration at the surface for a PP/PET 28/72 *P* and a PP/PET 86/14 *P* blend are determined as a function of moulding time under pressure (1/*x*/0 with $x = 2, 3, 5$ min) and annealing time (1/2/*x* with $x = 0$ and 5 min). Table 4 shows that both the concentration and the size of the dispersed

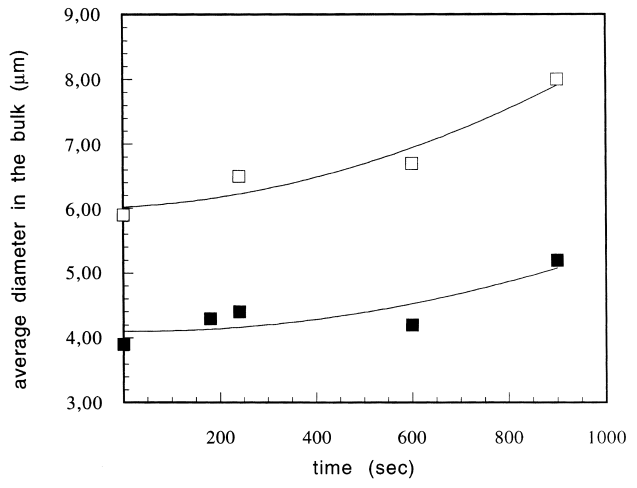

Fig. 8. Dispersed phase size in the bulk as function of time at 280°C where: □ is PP/PET 28/72 blends and ■ is PP/PET 86/14 blends. The coalescence of the dispersed phase has a small influence on the increases of average diameter under the time scales influenced.

Table 4
The dispersed phase size at the surface (D_s) and surface concentration (C_s) at various compression moulding times and this for a PP/PET 28/72 and a PP/PET 86/14 blend where PP and PET are the respective dispersed phases

Time	PP/PET 28/72 p		PP/PET 86/14 p	
	D_s (µm)	C_s (%)	D_s (µm)	C_s (%)
1/2/0	5.7	10.6	5.2	87.5
1/3/0	6.4	11.0	6.4	86.1
1/5/0	5.0	11.1	5.8	86.3
1/2/5	5.2	12.0	5.1	86.0

phase are independent of time. There is no significant evolution of the surface morphology with time. Longer compression moulding times could not be analysed because of PP degradation. During pressure increase the flow velocity is low.

3.3. Compression-moulded PP/PET films at high shear

Squeezing flow has been used to produce films where the starting morphology is sheared to a much larger extent (Fig. 9). Therefore blocks of the blend coming directly from the Brabender have been compression moulded with polyimide as moulding surface. The PP surface concentration corresponding to three different compositions (PP/PET 86/14 *B* 1/2/0, 78/22 *B* 1/2/0 and 28/72 *B* 1/2/0) and measured on two different zones of the samples (zones 1 and 8) are reported in Table 5. For comparison, the table also reports the results of the surface concentration for ground samples processed at low shear (see previous paragraph). The blend composition mentioned in Table 5 is the weight percentage added during melt mixing in the Brabender. The bulk concentration for the samples at low shear is lower than the blend composition due to the loss in dispersed phase during grinding.

3.3.1. PET dispersed phase

In Table 5, for blends with PET as dispersed phase (PP/PET 86/14, 78/22) and high shear the surface concentration of PP in zone 1 is lower than in the bulk and than that

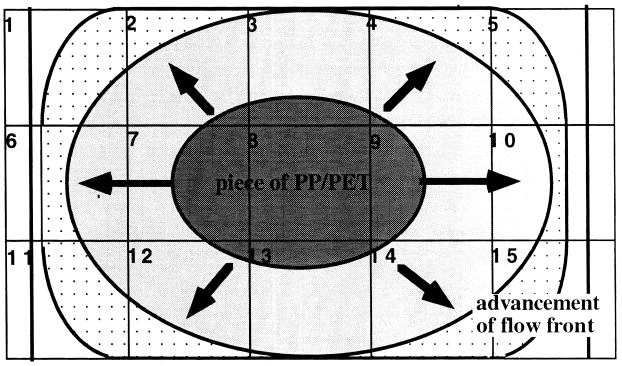

Fig. 9. Compression moulding of pieces directly coming from the Brabender. They are placed in the middle of the mould and sheared progressively during compression moulding. Zones 1 and 8 will be analysed.

Table 5
The PP surface and bulk concentration of PP/PET blends at three different compositions of films prepared by squeezing flow (PP/PET 86/14 *B* 1/2/0, 78/22 *B* 1/2/0 and 28/72 *B* 1/2/0). The surface has been analysed in two different zones: zone 1 and zone 8 (see Fig. 9). The table also mentions the results of the surface concentration for samples where the shear during processing was low

Blend composition	Dispersed phase	PP/PET *P* low shear Bulk (%PP)	PP/PET *B* high shear Surface (%PP)	Bulk (%PP)	Surface zone 1 (%PP)	Surface zone 8 (%PP)
28/72	PP	19.5	8.4	28	2.7	3.9
78/22	PET	83	84	78	70	84
86/14	PET	89	87	86	76	95

measured on films prepared at low shear. Micrographs of the same zone 1 (Figs 10 and 11) show that the dispersed phase at the surface is elongated into threads. Fig. 11 also shows that the bulk of the film remains undeformed.

Table 5 shows that for zone 8, the surface concentrations of PP for both blends are higher than in the bulk. The difference between the bulk and surface concentration is larger for compression-moulded films at high shear. The dispersed phase (PET) at the surface in zone 8 for PP/PET 86/14 is not elongated into threads but remains nodular.

The compression moulding induces a flow field where the shear rate at the surface is higher than in the bulk. The shear rate is also a function of the radial distance. We conclude that the morphology of the dispersed phase at the surface is clearly influenced by the flow velocity and this effect is restrained to the surface.

If, during the advancement of the flow front, a PET nodule makes contact with the surface, the increase of its surface with the polyimide is energetically favoured. The energy needed to deform the nodule against surface tension will be delivered by the flow field. In a way the PET is retained by the moulding surface and sheared into threads. The smaller the particles (surface tension/radius) the larger the energy required to deform the nodules on the surface into threads. This hypothesis is confirmed by the observation that in zones where the surface morphology is thread-like, the small nodules retain more or less their circular shape (Figs 10 and 11).

3.3.2. PP dispersed phase

When PP is the dispersed phase (PP/PET 28/72 *B* 1/2/0) the surface concentration for films prepared at high shear is

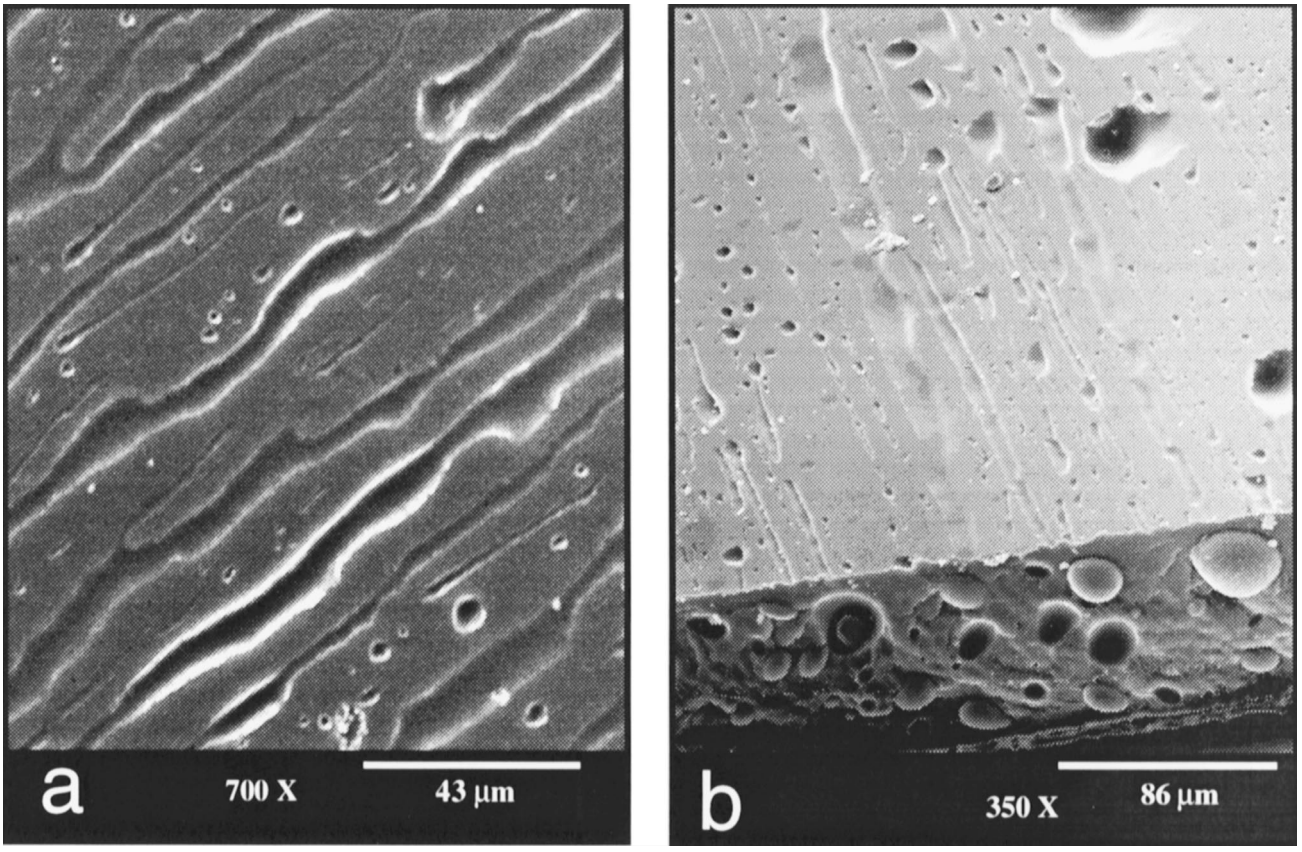

Fig. 10. Micrograph taken by SEM of the surface of a PP/PET 78/22 film, showing holes as the remainders of PET at the surface. The PET sticks to the moulding surface during demoulding. The dispersed phase can be seen to be strongly elongated in the flow direction.

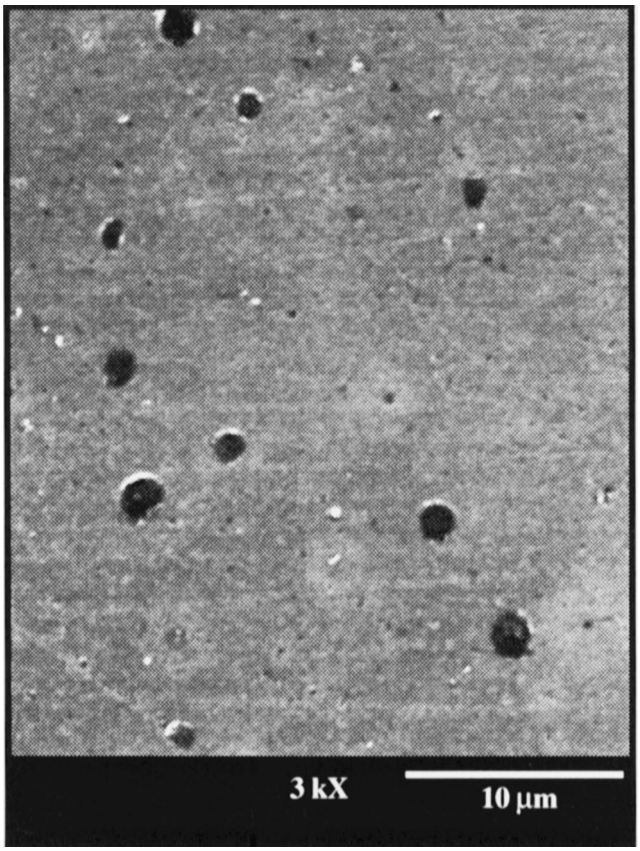

Fig. 11. SEM picture of a cryogenic fractured PP/PET 78/22 film, showing the PET in the bulk to be non-deformed while the PET at the surface is strongly elongated.

lower than for samples prepared at low shear (Table 5). The dispersed phase at the surface was not deformed but remained nodular all over the sample (Fig. 12). PP, having a lower surface energy then PET, has a tendency to go into the bulk in order to decrease its interfacial area with PI.

4. Conclusions

The aim of this work was to investigate the relation existing between the surface and the bulk morphology in heterogeneous polymer materials after compression moulding. The influence of blend composition and processing conditions have been examined, keeping the moulding surface constant.

It is found that when a very low shear is applied the bulk and surface morphologies are very similar. However, the difference of polarity between the moulding surface, the dispersed phase and the matrix phase induces a difference in dispersed phase size between the surface and bulk. The dispersed phase size at the surface is different than in the bulk. The difference can be attributed to the polarities of the moulding surface, the dispersed phase and the matrix. It is also shown that the concentration at the surface is equal to the bulk concentration when PET is the dispersed phase. This is not the case when PP is the dispersed phase, this has to be attributed to the experimental set up (loss of nodules). Finally for processing times shorter than 8 min no change of the dispersed phase size and of concentration at the surface is observed.

When the shear on the blend is high, the surface morphology is strongly influenced by the interplay between flow and the affinity of the dispersed phase for the contact surface while the bulk morphology remains undeformed. In the case where the dispersed phase (PET) has a higher affinity for the moulding surface than the matrix, the surface is enriched in dispersed phase and when there is no affinity for the moulding surface the dispersed phase (PP) shows a tendency to enter into the bulk.

In a following paper we will report on the influence of the polarity of the moulding surface. The influence of the blend viscosity ratio on the relation between surface and bulk morphologies will also be analysed.

Acknowledgements

A. Van Dooren is heartily acknowledged for the measurements of the surface energy of PP and PET. The authors also would like to thank Professor P. Rouxhet and Dr. B. Neysten for the most valuable discussions and corrections to the text. This work is partly supported by the programme ‘Biometrials’ of the Région Wallone of Belgium.

References

[1] Favis DB, Chalifoux JP. Polymer 1988;29:1791.
[2] Favis DB, Chalifoux JP. Polym Engng Sci 1987;27:1591.
[3] Favis DB, Willis JM. J Polym Sci: Part B Polym Phys 1990;28:2259.
[4] Wu S. Polym Engng Sci 1987;27:335.
[5] Serpe G, Jarrin J, Dawans F. Polym Engng Sci 1990;30:553.
[6] Xanthos M. Polym Engng Sci 1988;28:1392.
[7] Scott CE, Macosko CW. Polymer 1995;35:5422.
[8] Scott CE, Macosko CW. Polymer 1995;36:461.
[9] Guégan P, Macosko CW, Ishizone T, Hirao A, Nakahama S. Macromolecules 1994;27:4993.
[10] Marechal Ph. PhD thesis, Universite Catholique de Louvain, Belgium, 1993.
[11] De Roover B, Devaux J, Legras R. PAmXD,6PP-g-MA blends 3. Microstructure, blend melt viscosity and copolymer concentration relationship. J Polym Sci Part A: Polym Chem 1997;35(7):1313.
[12] Hubbell JA. Trends in Polymer Science 1994;2 (1):20.
[13] Shakesheff KM, Chen X, Davies MC, Domb A, Roberts CJ, Tendler SJB, Williams PM. Langmuir 1995;11:3921.
[14] Davies MC, Shakesheff KM, Shard AG, Domb A, Roberts CJ, Tendler SJB, Williams PM. Macromolecules 1996;29:2205.
[15] Takahara A, Korehise K, Ge SR, Kajiyama T. J Vac Sci Technol A 1994;15:2956.
[16] Bonnerup C, Gatenholm P. J Adhesion Sci Technol 1993;7:247.
[17] Cifra W. J Chem Phys 1991;96:157.
[18] Jones RAL, Kramer EJ. Polymer 1993;34:115.
[19] Harriharran A, Kumar SK, Russell TP. Macromolecules 1991;24:4909.
[20] Kumar SK, Russell TP. Macromolecules 1992;24:3816.

[21] Sakellariou P. Polymer 1993;34 (16):3408.
[22] Occhiello E, Garbassi F. Macromol Symp 1994;78:131.
[23] Schmidt JJ, Gardella JA Jr, Salvati L Jr. Macromolecules 1889;22:4489.
[24] Pan DH-K, Prest WM Jr. J Appl Phys 1985;58 (8):2861.
[25] Clark MB Jr, Burkhardt CA, Gardella JA Jr. Macromolecules 1989;22:4495.
[26] Clark MB Jr, Burkhardt CA, Gardella JA Jr. Macromolecules 1991;24:799.
[27] Schmitt RL, Gardella JA Jr, Salvati L Jr. Macromolecules 1986;19:648.
[28] Guckenbiehl B, Stamm M, Springer T. Colloids and Surfaces A. 1994;86:311.
[29] Cowie JMG, Devlin BG, McEwen IJ. Polymer 1993;34:4130.
[30] Hong PP, Boerio FJ, Smith SD. Macromolecules 1994;27:596.
[31] Bhatia QS, Pan DH, Koberstein JT. Macromolecules 1988;21:2166.
[32] Jackson ST, Short RD. J Mater Chem 1992;2 (2):259–260.
[33] Short R, Ameen AP, Jackson ST, Pawson DJ, O'Toole L, Ward AJ. Vacuum 1993;44 (11):1143–1160.
[34] Davies MC, Shakesheff KM, Shard AG, Domb A, Roberts CJ, Tendler SJB, Williams PM. Macromolecules 1996;29:2205.
[35] Briggs D. Spectrosc Eur 1993;5:8.
[36] Jackson ST. PhD thesis, University of Sheffield, 1992.
[37] Briggs D, Fletcher IW, Reichmaier JL, Agulo-Sanchez RD. Short Surf Interface Anal 1996;24:419.
[38] Kumacheva E, Li L, Winnik MA, Shinozaki DM, Cheng PC. Langmuir 1997;13:2483.
[39] Tanaka K, Yoon JS, Takahara A, Kajiyama T. Macromolecules 1995;28:934.
[40] Tanaka K, Takahara A, Kajiyama T. Macromolecules 1996;29:3232.
[41] Walheim S, Böltau M, Mlynek J, Krausch G, Steiner U. Macromolecules 1997;30:4995.
[42] Bhatia QS, Burell MC, Chera JJ. J Appl Polym Sci 1992;46:1915.
[43] Nysten B, Verfaillie G, Ferain E, Legras R, Lhoest JB, Poleunis C, Betrand P. Microsc Micoanal Microstruct 1994;5:373.
[44] Mack GL. J Phys Chem 1936;40:159.
[45] Bartell FE, Zuidema HH. J Am Chem Soc 1936;58:1449.
[46] Wu WA. J Paint Techn 1972;44:546.
[47] Brandrup J, Immergut EH. Polymer handbook, pp. V-23, V-71. New York: John Wiley and Sons, 1975.
[48] Wu S. Polymer interface and adhesion, pp. 67–132. New York: Marcel Dekker Inc., 1986.
[49] Favis DB. J Appl Polym Sci 1990;39:285.
[50] Fortelny I, Kovar J. Polymer Composites 1988;9 (2):119.